

Lewis Acids

The Reactivity of Isomeric Nitrenium Lewis Acids with Phosphines, Carbenes, and Phosphide

Diya Zhu,^[a] Zheng-Wang Qu,^{*[b]} Jiliang Zhou,^[a] and Douglas W. Stephan^{*[a]}

Abstract: Alkylation of spiro[fluorene-9,3'-indazole] at N(1) and N(2) with *t*BuCl affords the nitrenium cations $[\text{C}_6\text{H}_4\text{N}_2(\text{tBu})\text{C}(\text{C}_{12}\text{H}_8)]^+[\text{BF}_4]^-$, **1** and **2**, respectively. Compound **1** converts to **2** over the temperature range 303–323 K with a free energy barrier of $28 \pm 5 \text{ kcal mol}^{-1}$. Reaction of **1** with PMe_3 afforded the *N*-bound phosphine adduct $[\text{C}_6\text{H}_4\text{N}(\text{tBu})\text{N}(\text{PMe}_3)\text{C}(\text{C}_{12}\text{H}_8)]^+[\text{BF}_4]^-$ **3**. However, phosphines attack **2** at the *para*-carbon atom of the aryl group with concurrent cleavage of N(2)–C(1) bond and proton migration to C(1) affording $[(\text{R}_3\text{P})\text{C}_6\text{H}_3\text{NN}(\text{tBu})\text{CH}(\text{C}_{12}\text{H}_8)]^+[\text{BF}_4]^-$ (*R* = Me **4**,

*n*Bu **5**). Analogous reactions of **1** and **2** with the carbene SIMes prompt attack at the *para*-carbon with concurrent loss of H^+ affording the radical cation salts $[(\text{SIMes})\text{C}_6\text{H}_3\text{N}(\text{tBu})\text{NC}(\text{C}_{12}\text{H}_8)]^+[\text{BF}_4]^-$ **6** and $[(\text{SIMes})\text{C}_6\text{H}_3\text{NN}(\text{tBu})\text{C}(\text{C}_{12}\text{H}_8)]^+[\text{BF}_4]^-$ **7**, whereas reaction of **2** with BAC gives the Lewis acid-base adduct, $[\text{C}_6\text{H}_4\text{N}(\text{BAC})\text{N}(\text{tBu})\text{C}(\text{C}_{12}\text{H}_8)]^+[\text{BF}_4]^-$ **8**. Finally, reactions of **1** and **2** with KPPH_2 result in electron transfer affording $(\text{PPH}_2)_2$ and the persistent radicals $\text{C}_6\text{H}_4\text{N}(\text{tBu})\text{NC}(\text{C}_{12}\text{H}_8)^+$ and $\text{C}_6\text{H}_4\text{NN}(\text{tBu})\text{C}(\text{C}_{12}\text{H}_8)^+$. The detailed reaction mechanisms are also explored by extensive DFT calculations.

Introduction

The classification of electron donors and acceptors as bases and acids, respectively delineated by Lewis in the 1920s is a concept that permeates much of chemistry.^[1] Indeed, this concept remains relevant today as one of the underpinnings of coordination and main group chemistry. Moreover, built on perturbations to Lewis' fundamental notion, the concepts of „umpolung“^[2,3,4–11] and „frustrated Lewis pairs (FLPs)“^[12–16] have led to new and unique approaches to synthetic and catalytic chemistry. The combination of these latter two concepts has unveiled new Lewis acids for FLP chemistry. For example, in 2013, we described the development of highly electrophilic phosphonium cations (EPCs) for the activation of C–F bonds.^[17] Moreover, those Lewis acids based on phosphorus, an element traditionally used in Lewis donors, proved useful in

FLP hydrogenations, transfer hydrogenations and hydrosilylations.^[18]

In a similar sense, nitrogen-containing compounds usually feature an accessible lone pair at the N atom, and thus act as Lewis bases. Nonetheless, there are known examples of *N*-centered electrophiles.^[19–23] One class of such nitrogen-centered electrophiles, nitrenium ions has drawn recent attention. In seminal work, Gandelman showed that a triazinium salt (*N*-heterocyclic nitrenium (NHN)) can form classic Lewis acid/base adducts with phosphines (Figure 1). Gandelman and co-workers have also expanded the range of triazolium salts, demonstrating access to a wide variety of N-based Lewis acids.^[24–27] More recently, Mehta and Goicoechea^[28] as well as Gandelman^[29]

[a] D. Zhu, Dr. J. Zhou, Prof. Dr. D. W. Stephan
Department of Chemistry
University of Toronto
80 St George St, Toronto, Ontario, M5S3H6 (Canada)
E-mail: dstephan@chem.utoronto.ca

[b] Dr. Z.-W. Qu
Mulliken Center for Theoretical Chemistry
Institut für Physikalische und Theoretische Chemie
Rheinische Friedrich-Wilhelms-Universität Bonn
Beringstrasse 4, 53115 Bonn (Germany)
E-mail: qu@thch.uni-bonn.de

Supporting information and the ORCID identification number(s) for the author(s) of this article can be found under:
<https://doi.org/10.1002/chem.202004798>.

© 2020 The Authors. Chemistry - A European Journal published by Wiley-VCH GmbH. This is an open access article under the terms of the Creative Commons Attribution License, which permits use, distribution and reproduction in any medium, provided the original work is properly cited.

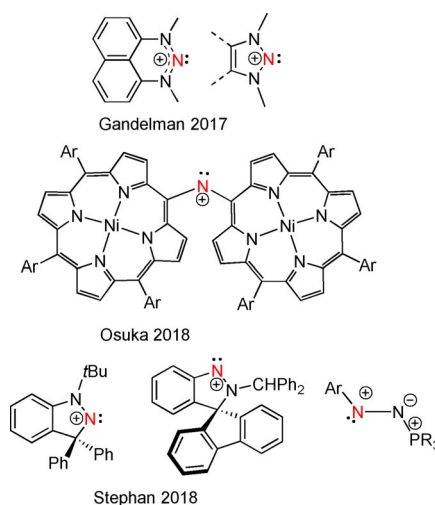


Figure 1. Recent examples of nitrenium cation-based Lewis acids.

have exploited the Lewis acidity of triazinium salts for Lewis acid catalysis and FLP Si–H activation.

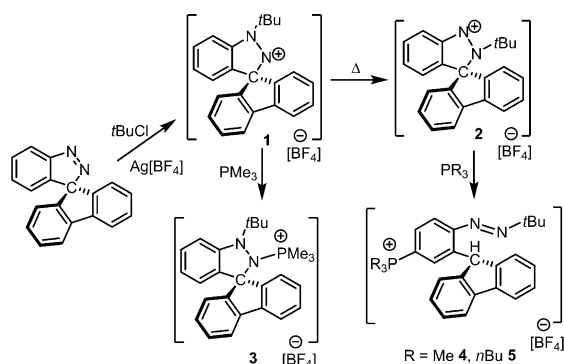
In a concurrent effort, Osuka and co-workers have described the synthesis of a stable diporphyrinylaminyl nitrenium cation.^[30] Moreover, they showed that this species was prepared by stepwise oxidation of the corresponding diporphyrinylamine through a stable aminyl radical.

In our own efforts, we developed a cyclic (amino)(alkyl)nitrenium (CAAN) cation that exhibited enhanced electrophilicity (Figure 1)^[31] forming Lewis adducts or participating in FLP reactivity when combined with phosphines or carbenes. This finding was also consistent with a computational study that found annulation to be an effective way to stabilize cyclic nitrenium ions.^[32] More recently, we also reported that alkylation of spiro[fluorene-9,3'-indazole] with Ph₂CHCl affords a nitrenium cation that is indeed Lewis acidic at nitrogen.^[33] Interestingly, upon deprotonation of the benzylic carbon, the resulting zwitterion exhibits Lewis basicity at the nitrogen atom that was formerly acidic. In addition, we demonstrated that diazonium cations of the form [ArN₂(PR₃)]⁺ are N-based Lewis acids and behave as one or two electron acceptors, yielding the corresponding radical and Lewis acid-base adducts, respectively.^[34]

In the present work, we further examine more steric-hindered Lewis acidic nitrenium cations illustrating that alkylation of the N(1)-position of fluorene-9,3'-indazole with a *tert*-butyl group provides access to a nitrenium cation that thermally isomerizes to N(2)-alkylated isomer. Moreover, these nitrenium cations exhibit diverse reactivity upon combination with donors such as phosphine, carbene, and phosphide. The observed products are shown to depend on both the steric demands and basicity of the donors.

Results and Discussion

Reaction of the spiro[fluorene-9,3'-indazole] with *t*BuCl and Ag[BF₄] in CH₂Cl₂ at room temperature generates two products, **1** and **2** (Scheme 1). Under these conditions, **2** is the dominant product containing about a 1: 2.6 ratio of **1**: **2**. After work-up, these salts were separated by recrystallization from a saturated CH₂Cl₂/pentane solution at –35 °C with the bright orange product **1** precipitating first in 24% yield and the sandy orange product **2** requiring higher concentrations of



Scheme 1. Synthesis of **1**–**5**.

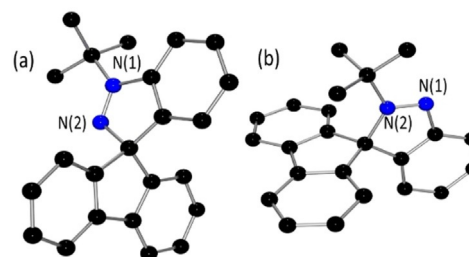


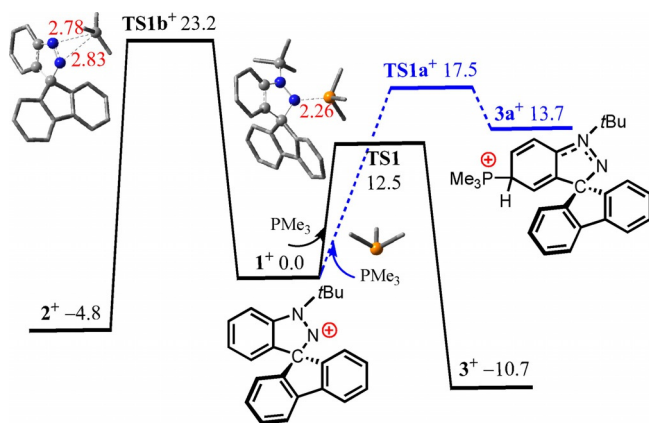
Figure 2. POV-ray depictions of cations (a) **1** and (b) **2**; hydrogen atoms and BF₄ anions are omitted for clarity. C: black; N: blue. Selected bond lengths: (a) N(1)–N(2) 1.263(5), (b) N(1)–N(2) 1.265(3) Å.

pentane was isolated in 65% yield. These products are readily distinguished by ¹H NMR spectra and they show distinct resonances at 1.54 and 2.61 ppm attributable to the *t*Bu groups of **1** and **2**, respectively.

Crystallographic studies (Figure 2) confirmed the product salts as [C₆H₄N(*t*Bu)N(C₁₂H₉)] [BF₄][–] **1** and [C₆H₄NN(*t*Bu)C(C₁₂H₉)] [BF₄][–] **2**, which are isomers in which alkylation occurred at the N(1) and N(2) positions, respectively. The metric parameters in the two isomers were similar. For example, the N(1)–N(2) bond lengths in **1** and **2** were found to be 1.263(5) and 1.265(3) Å, respectively, slightly longer than typical N=N double bonds. However, the difference between the torsion angles of N(1)–N(2)–C(1)–C(19) in **1** (124.4(3)°) and N(1)–N(2)–C(1)–C(15) in **2** (128.2(2)°) is consistent with variations in the steric conflict between the bulky fluorene and the *t*Bu-substituent. In contrast to previously reported CAANs,^[31,33] compound **1** was observed to slowly convert to **2** in solution at ambient temperature. The initial rates observed for this isomerization was carefully monitored by ¹H NMR spectroscopy. The rate of formation of **2** showed a first order dependence on the concentration of **1** (see Figure S32 in the Supporting Information). While the solubility of **1** limited the temperature range accessible, an Eyring plot analysis was performed with kinetic data collected over the temperature range 303–323 K, with the free energy Δ*G* (activation enthalpy Δ*H*) barrier of the isomerization determined as 28 ± 5 (34 ± 3) kcal mol^{–1}.

To further probe the mechanistic implications of these kinetic data, DFT calculations at the PW6B95-D3/def2-QZVP + OSOMO-RS//TPSS-D3/def2-TZVP + COSMO level of theory in CHCl₃ solution^[35–49] was undertaken (see the Supporting Information). Both salts **1** and **2** should exist as separated ion pairs **1**⁺ and **2**⁺, respectively (see Computational details in the Supporting Information). The conversion from cation **1**⁺ to **2**⁺ is –4.8 kcal mol^{–1} exergonic over a free energy (activation) barrier of 23.2 (32.6) kcal mol^{–1} via a 1,2 *tert*-butyl-migration (via transition structure **TS1b**⁺, Scheme 2), in excellent agreement with the kinetic experimental data.

The nature of the LUMOs in the isomeric cations **1** and **2** was probed computationally (Figure 3). In both cases, the LUMOs consist of the π* orbital mainly located on the conjugated N=N bond and its adjacent aryl ring. Given that these contributions to the Lewis acidity of **1** and **2** have distinctly different degrees of steric congestion at nitrogen centers, divergent reactivity toward nucleophiles can be expected.



Scheme 2. DFT-computed free energy paths (in kcal mol⁻¹, at 298 K and 1 mol L⁻¹) of the reaction of cation **1**⁺ with PMe₃.

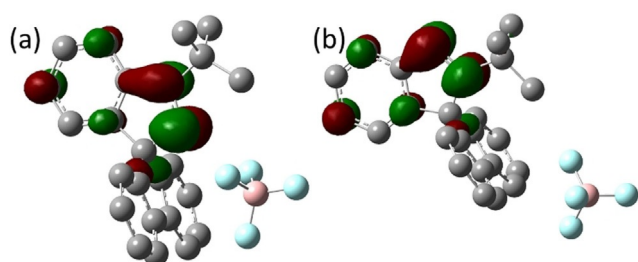


Figure 3. Depictions of the LUMOs of (a) **1**, (b) **2** in CHCl₃ solution; computed at the TPSS-D3/def2-TZVP + COSMO level.

To begin to probe this possibility, reactions of these nitrenium cations with phosphine and carbene donors were probed. Initially, **1** was exposed to an excess amount of PMe₃. Upon addition, the intensely orange solution of **1** faded to colorless immediately. A white solid **3** was isolated in 95% yield. The ³¹P NMR spectrum of **3** showed a signal at 64.6 ppm, which is similar to that seen for previously reported CAAN-phosphine adducts.^[31,33] Indeed the coordination of phosphine to nitrogen with the pyramidalization of nitrogen atom in [(C₆H₄N(tBu)N(PMe₃)C(C₁₂H₈))[BF₄]] **3** was confirmed by an X-ray diffraction study (Scheme 1, Figure 4). The resulting N–P distance was found to be 1.679(3) Å which is similar to that reported for [(C₆H₄(tBu)NN(PMe₃)C(C₆H₅)₂)⁺ (1.693(3) Å),^[31] [(C₁₂H₈)(Ph₂CH)NN(C₆H₄)(PMe₃)⁺ (1.686(2) Å)^[33] and typical of N–P single bonds.^[51]

The analogous treatment of **2** with PMe₃ afforded a tan solid **4** in 92% yield after workup (Scheme 1). The ³¹P{¹H} NMR spectrum of **4** revealed a sharp singlet at 22.0 ppm while the ¹H NMR spectrum showed a new resonance appearing at 6.21 ppm. Further, 2D HSQC NMR spectroscopic data affirmed the correlation of this proton signal with the resonances at 47.2 ppm in the ¹³C{¹H} NMR spectrum arising from a sp³ carbon atom. Repeated efforts to characterize **4** by X-ray crystallographic methods gave consistently poor quality crystals, although diffraction data confirmed the connectivity in which phosphine is bound to the carbon atom *para*- to N with con-

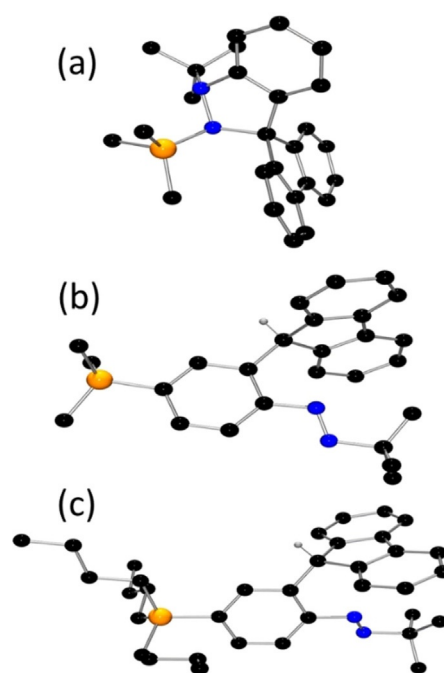
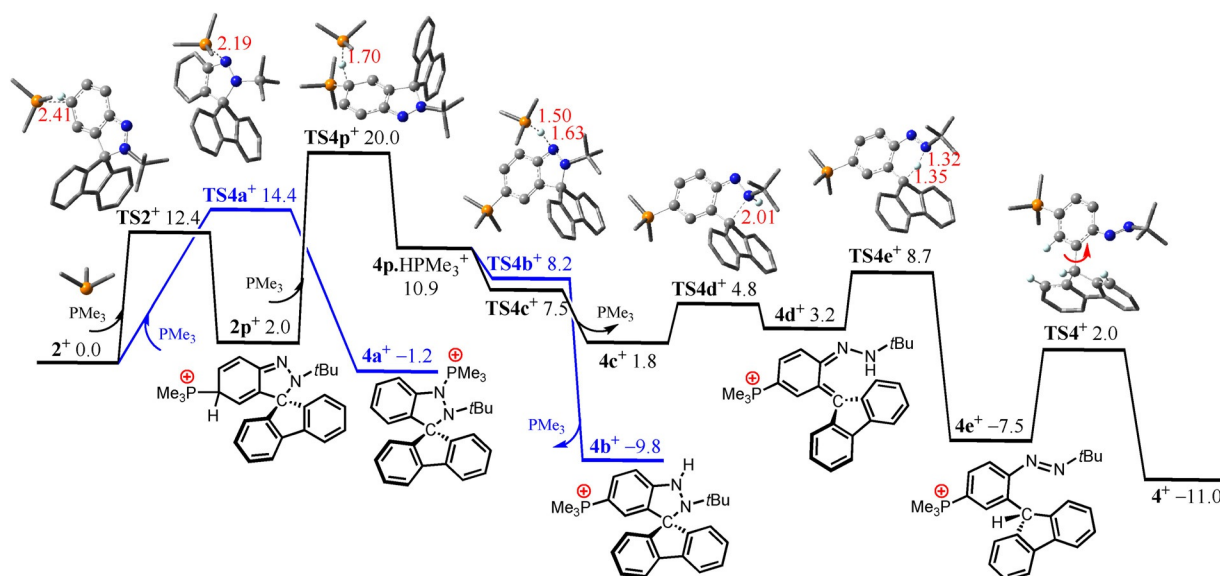


Figure 4. POV-ray depictions of cations (a) **3**, (b) **4**, and (c) **5**; hydrogen atoms and BF₄ anions are omitted for clarity. C: black; N: blue; P: orange. Selected bond lengths: **3**: N(1)–N(2) 1.470(4), N(1)–P(1) 1.679(3) Å; **5**: N(1)–N(2) 1.228(5), C(5)–P(1) 1.783(5) Å.

current cleavage of N(2)–C bond and proton migration affording [(Me₃P)C₆H₃NN(tBu)CH(C₁₂H₈))[BF₄]] **4** (Figure 4).

In a similar fashion, addition of *n*Bu₃P to **2** resulted phosphonium diazo salt **5** in 95% yield (Scheme 1). The crystallographic study confirmed the formulation as [(*n*Bu₃P)C₆H₃NN(tBu)CH(C₁₂H₈))[BF₄]]. With two molecules in the asymmetric unit, the average N–N bond length was determined to be 1.232(5) Å, while the P–C distances were found to be 1.783(5) and 1.802(5) Å. It is noteworthy that the nucleophilic attack at the carbon *para*- to the Lewis acidic N(1) in **2** is reminiscent of the reaction of bulky phosphines with B(C₆F₅)₃ in which the donor attack *para*- to the Lewis acidic boron affording the phosphonium-borate zwitterions, (R₃P)C₆F₄B(C₆F₅)₂F.^[52,53]

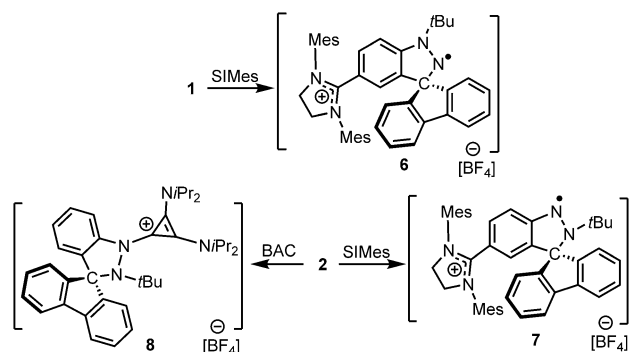
To garner further insight, the free energy paths of the reactions of both salts **1** and **2** with phosphine PMe₃ in CHCl₃ solution were computed at the PW6B95-D3/def2-QZVP + COSMORS//TPSS-D3/def2-TZVP + COSMO level of theory. The reaction of cation **1**⁺ with PMe₃ was computed to proceed via the direct P⋯N nucleophilic attack at the N(2)-site to give the stable Lewis acid-base adduct **3**, which is –10.7 kcal mol⁻¹ exergonic over a low free energy barrier of 12.5 kcal mol⁻¹ (via **TS1**, Scheme 2). The alternative P⋯C nucleophilic attack at the aryl *para*-carbon is 13.7 kcal mol⁻¹ endergonic over a barrier that is 5.0 kcal mol⁻¹ higher (via **TS1 a**⁺) to give the adduct **3 a**. Further deprotonation of **3 a** with PMe₃ is unlikely due to an additional barrier of 21.0 kcal mol⁻¹ (see the Supporting Information). It is noteworthy that the formation of **3** is also kinetically 10.7 kcal mol⁻¹ favored over the isomerization of **1** to **2** (1,2-shift of *t*Bu via **TS1 b**⁺).



Scheme 3. DFT-computed free energy paths (in kcal mol⁻¹, at 298 K and 1 mol L⁻¹) for the reaction of cation **2**⁺ with PMe₃.

Computations for the corresponding reaction of the cation **2**⁺ with PMe₃ show that nucleophilic attack at the N(1)-site is only -1.2 kcal mol⁻¹ exergonic over a low barrier of 14.4 kcal mol⁻¹ (via **TS4a**⁺) and thus reversible at ambient temperature (Scheme 3). On the other hand, the nucleophilic attack by PMe₃ at the aryl *para*- to N is 2.0 kcal mol⁻¹ endergonic over barrier that is 2.0 kcal mol⁻¹ lower in energy (via **TS2**⁺) yielding the transient adduct **2p**⁺. Deprotonation by additional PMe₃ is 8.9 kcal mol⁻¹ endergonic over a moderate barrier of 18.0 kcal mol⁻¹ (via **TS4p**⁺) However, the resulting transient phosphonium-complex **4p**, can mediate protonation of at the basic *N*-sites with an overall barrier of 21.2 kcal mol⁻¹ due to reversibly formed adduct **4a**⁺. Protonation at the N(1)-site is barrierless but and -20.7 kcal mol⁻¹ exergonic giving the cation **4b**⁺ and free PMe₃. Alternatively, protonation at the N(2)-site (via **TS4c**⁺) is also barrierless, prompting proton transfer to carbon, C–N bond cleavage rotation of 9-fluorenyl group to give the cation of **4**.

To further exploit these cations, **1** was also reacted with 1,3-bis(2,4,6-trimethylphenyl)-4,5-dihydroimidazol-2-ylidene (SIMes) yielding a purple species **6** at 67% yield (Scheme 4). The



Scheme 4. Synthetic routes to **6**–**8**.

¹H NMR spectrum of **6** is silent and attempts to characterize radical **6** by X-ray crystallography were fruitless. However, the EPR spectrum of **6** was recorded and simulated revealing a *g* value of 2.0049 of which hyperfine couplings of N: 11.50, 4.18, 0.98, 0.33 G and H: 0.59, 0.41, 0.21 G (Figure 5). The corresponding reaction of the *N*-Lewis acid **2** with the carbene SIMes was performed in *o*-C₆F₂H₄ affording a red species **7** at 80% yield. The ¹H NMR spectrum of **7** is also silent, while the EPR spectrum of **7** was similar to that of **6** with a *g* value of 2.0042 and hyperfine couplings of N: 9.39, 6.67, 0.48, 0.39 G, and H: 2.67, 0.60, 0.53 G (Figure 5). Single crystals for X-ray diffraction analysis were obtained by layering of pentane into a THF solution of **7** at -35 °C. The solid-state structure revealed the formulation of **7** as [(SIMes)C₆H₃NN(*t*Bu)C(C₁₂H₈)]⁺[BF₄]⁻ (Figure 6). The N–N bond length in **7** was found to be 1.350(3) Å, which is longer than that seen in **2**. The unambiguous characterization of **7** suggests an analogous structure for **6** (i.e. [(SIMes)C₆H₃N(*t*Bu)NC(C₁₂H₈)]⁺[BF₄]⁻). Indeed, the liberation of H₂ was confirmed by NMR spectroscopy of the reaction mixtures in a sealed NMR tube in C₆D₆.

Compound **2** was also reacted with the sterically smaller, yet more basic carbene, bis(diisopropylamino)-cyclopropenylidene (BAC), at room temperature. This yielded a black solid **8** in

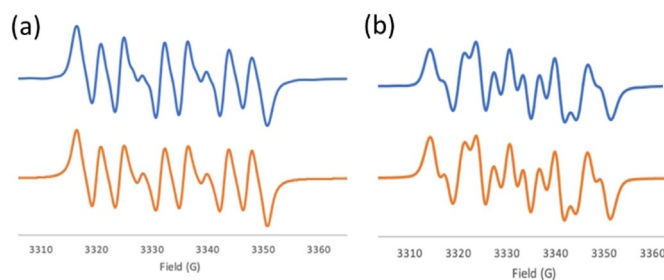


Figure 5. Observed (blue) and simulated (orange) EPR spectra for (a) **6** and (b) **7**.

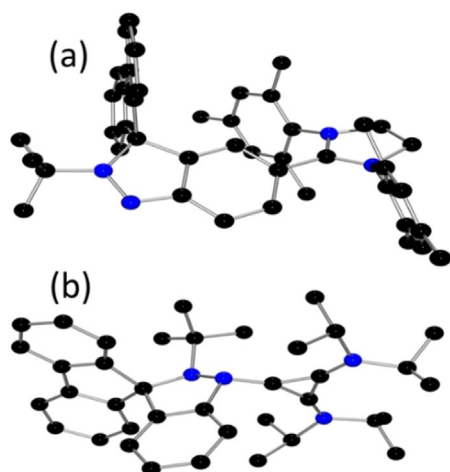


Figure 6. POV-ray depictions of cations (a) **7** and (b) **8**; hydrogen atoms and BF_4^- anions are omitted for clarity. C: black; N: blue. Selected bond lengths: **7**: N(1)–N(2) 1.350(3), C(6)–C(24) 1.461(4) Å; **8**: N(1)–N(2) 1.505(6), N(1)–C(24) 1.404(7) Å.

78% yield. While the NMR data was consistent with the combination of the two reagents, an X-ray crystallographic study confirm the formulation of **8** as $[\text{C}_6\text{H}_4\text{N}(\text{BAC})\text{N}(\text{tBu})\text{C}(\text{C}_{12}\text{H}_8)]^+[\text{BF}_4]^-$ (Figure 6). In this species, the BAC is coordinated to the electrophilic N(1)-site leading to pyramidalization of nitrogen atoms and an N–N bond length of 1.505(6) Å. The newly formed N–C bond length was found to be 1.404(7) Å, which is significantly longer than those seen in the carbene-stabilized nitrogen cation, $[(\text{BAC})_3\text{N}]^{3+}$ (1.378(3) Å) reported by Alcarazo and co-workers.^[54]

The formation of the radical cations in **6** and **7** suggests that steric demands preclude nucleophilic attack of SIMes at the Lewis-acidic N(1) site, instead prompting attack at the aryl *para*-carbon. While this aspect is analogous to the formation of **4** and **5**, the strong σ donation from carbene prompts loss of a H-atom affording H_2 and the radical cations. Presumably in the case of BAC, the significantly lesser steric demand results in the classical donor–acceptor bond between the carbene and the Lewis acidic nitrenium cation.

Interestingly, compounds **6** and **7** exhibit reversible redox behavior at -0.29 and -0.14 V, respectively, as evidenced by the cyclic voltammetry in $o\text{-C}_6\text{F}_2\text{H}_4$ containing 0.085 M $n\text{Bu}_4\text{NPF}_6$ as a supporting electrolyte (Figures 7 and S42). These were attributed to the facile oxidation of the radical cations to the corresponding dication, reminiscent of the oxidation of aminyl radical reported by Osuka^[30] and pyridinyl radicals by Hansman.^[55] Compound **7** showed a second reversible redox wave at -1.14 V attribute to the reduction of the cation to the corresponding neutral zwitterionic species.^[56] A further reduction of this species is irreversible at -2.47 V. In contrast, compound **6** is reduced irreversibly at about -1.4 V. The high reversible nature of the reduction of **7** are attributed to the stabilization of the zwitterionic species by the adjacent π -system (Scheme 5).

In related efforts compound **1** or **2** were treated with 1 equiv of KPPH_2 in THF. This prompted the immediate color

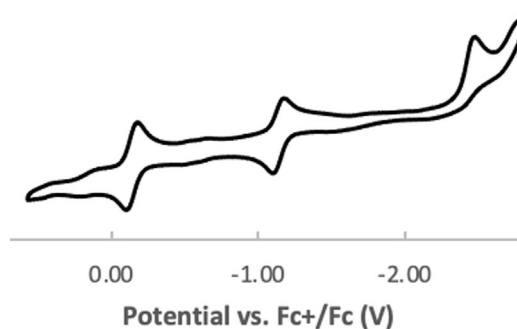
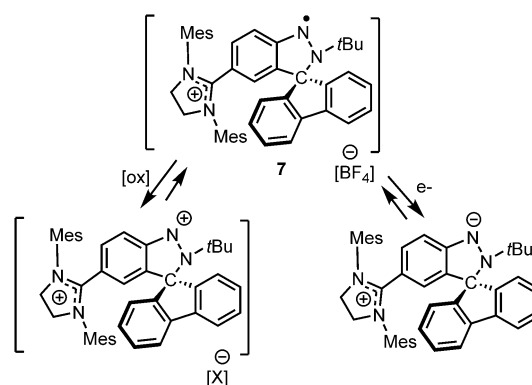
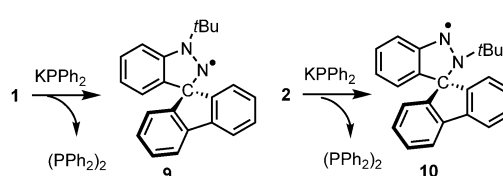


Figure 7. Cyclic voltammogram of compound **7** recording by using $[n\text{Bu}_4\text{N}][\text{BF}_4]$ as the electrolyte and ferrocene as the standard.



Scheme 5. Redox reactivity of **7**.

change to a deep green color while the $^{31}\text{P}\{^1\text{H}\}$ spectrum of the reaction crude showed the formation of $(\text{Ph}_2\text{P})_2$ (Figures S35 and S37). Monitoring the reactions by EPR spectroscopy showed signals suggesting the formation of the respective radicals **9** and **10**. These observations suggest a net electron transfer from phosphide to the corresponding nitrenium-cation and thus the formulations of **9** and **10** as the aminyl radicals $\text{C}_6\text{H}_4\text{N}(\text{tBu})\text{NC}(\text{C}_{12}\text{H}_8)^\bullet$ and $\text{C}_6\text{H}_4\text{NN}(\text{tBu})\text{C}(\text{C}_{12}\text{H}_8)^\bullet$, respectively. EPR data for these species were consistent with *g* values of 2.0038 and 2.0037 for **9** and **10**, respectively (Figures S36 and S38). In addition, spectral simulations revealed hyperfine couplings to two N atoms and four hydrogen atoms, consistent with these formulations (Scheme 6, Figure 8, see the Supporting Information). While these radicals were not isolable in analytically pure form as only spiro[fluorene-9,3'-indazole] was recovered, these formulations were further supported by the observation of a reversible reductions in the cyclic voltammograms of **1** and **2** at ca. -0.70 and -0.54 V vs. Fc^+/Fc , re-



Scheme 6. Reactivity of **1** and **2** with KPPH_2 .

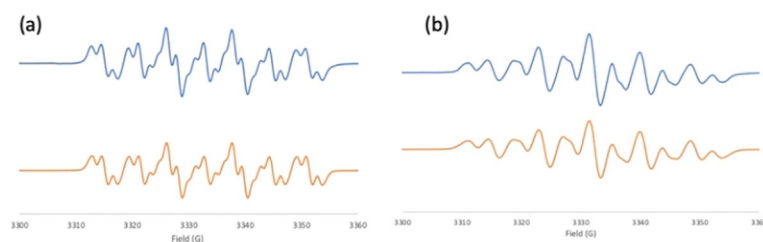


Figure 8. Experimental (blue) and simulated (orange) X-band EPR spectra of (a) **9** and (b) **10**.

spectively (see Figures S40 and S41 in the Supporting Information).

The reaction of **1** and **2** with phosphines and carbenes suggests that the reactions with phosphide could involve nucleophilic attack at either the electrophilic *N*-positions or at the *para*-carbon atom. It is noteworthy that in related work, Gandelman et al.^[27] recently described the analogous reaction involving a N-based Lewis acid derived from a triazolium derivative with phosphide suggesting that this proceeds via a transient nitrenium-phosphide adduct. However, DFT calculations for the present reactions of **1** and **2** with dimer (KPPH₂)₂ show that the initial electron transfer effects the reductions affording K(PPH₂)₂^{•−} and **9** and **10** respectively are exothermic by 4.5 and 8.0 kcal mol^{−1} reductions, while further electron transfer to **1** or **2** affording (PPH₂)₂ is even more exothermic (−60 kcal mol^{−1}) (see the Supporting Information).

Conclusions

Alkylation of spiro[fluorene-9,3'-indazole] with *t*BuCl affords the product of alkylation at the N(1) position, **1**, which undergoes a thermal rearrangement to give alkylation at N(2), **2**. While experimental and computational data show that each of these species are nitrenium cation salts, reactions of these species with various donors demonstrates Lewis acidity at both the nitrenium *N*-atom and the aryl carbon *para*-to N. For example, **1** binds PMe₃ at the Lewis acidic N(2) center to give **3**, while **2** reacts with phosphines at the *para*-carbon resulting in proton migration to carbon affording **4** and **5**. The bulky, yet stronger donor carbene, SIMes, reacts with **1** or **2** at the *para*-carbon, inducing loss of H⁺ to give NHC-substituted radical cations **6** and **7**. In contrast, the smaller carbene nucleophile, BAC, reacts with **2** to form the classical adduct **8** at the electrophilic N atom. Finally, in reactions of **1** and **2** with KPPH₂, electron transfer affords the (PPH₂)₂ and the corresponding diazo-radicals **9** and **10**. The access to one and two electron chemistry derived from these nitrenium cation-based Lewis acids augurs well for the development of a rich chemistry of N-based Lewis acids. We are continuing to explore related systems, with a particular interest in the applications in FLPs and Lewis acid catalysis.

Experimental Section

Crystallographic data: Deposition number(s) 2035309, 2035310, 2035311, 2035312, 2035313, 2035314, and 2035315 contain the supplementary crystallographic data for this paper. These data are

provided free of charge by the joint Cambridge Crystallographic Data Centre and Fachinformationszentrum Karlsruhe Access Structures service.

Acknowledgements

D.W.S. is grateful to NSERC of Canada for research support and the award of an NSERC Canada Research Chair and to the Guggenheim Foundation for a 2020 Guggenheim Fellowship. D.Z. is grateful to Dr. Alan Lough for the structure of compound **4** and the NMR facility at the University of Toronto for help and support. Z.W.Q. thanks the German Science Foundation (DFG) for financial support (Gottfried Wilhelm Leibnitz prize to Prof. Stefan Grimme). Open access funding enabled and organized by Projekt DEAL.

Conflict of interest

The authors declare no conflict of interest.

Keywords: carbenes • N-Lewis bases • phosphides • phosphines • radicals

- [1] G. N. Lewis, *Valence and the Structure of Atoms and Molecules*, Chemical Catalogue Company, New York, 1923.
- [2] D. Seebach, *Angew. Chem. Int. Ed. Engl.* **1979**, *18*, 239–258; *Angew. Chem.* **1979**, *91*, 259–278.
- [3] D. Seebach, D. Enders, *Angew. Chem. Int. Ed. Engl.* **1975**, *14*, 15–32; *Angew. Chem.* **1975**, *87*, 1–18.
- [4] X. Bugaut, F. Glorius, *Chem. Soc. Rev.* **2012**, *41*, 3511–3522.
- [5] D. W. Stephan, *Angew. Chem. Int. Ed.* **2017**, *56*, 5984–5992; *Angew. Chem.* **2017**, *129*, 6078–6086.
- [6] D. Enders, O. Niemeier, A. Henseler, *Chem. Rev.* **2007**, *107*, 5606–5655.
- [7] D. M. Flanigan, F. Romanov-Michailidis, N. A. White, T. Rovis, *Chem. Rev.* **2015**, *115*, 9307–9387.
- [8] M. N. Hopkinson, C. Richter, M. Schedler, F. Glorius, *Nature* **2014**, *510*, 485–496.
- [9] V. Nair, R. S. Menon, A. T. Biju, C. R. Sinu, R. R. Paul, A. Jose, V. Sreekumar, *Chem. Soc. Rev.* **2011**, *40*, 5336–5346.
- [10] M. H. Wang, K. A. Scheidt, *Angew. Chem. Int. Ed.* **2016**, *55*, 14912–14922; *Angew. Chem.* **2016**, *128*, 15134–15145.
- [11] C. Zhang, J. F. Hooper, D. W. Lupton, *ACS Catal.* **2017**, *7*, 2583–2596.
- [12] A. R. Jupp, D. W. Stephan, *Trends Chem.* **2019**, *1*, 35–48.
- [13] D. W. Stephan, *Science* **2016**, *354*, aaf7229.
- [14] D. W. Stephan, G. Erker, *Angew. Chem. Int. Ed.* **2015**, *54*, 6400–6441; *Angew. Chem.* **2015**, *127*, 6498–6541.
- [15] D. W. Stephan, *J. Am. Chem. Soc.* **2015**, *137*, 10018–10032.
- [16] D. W. Stephan, *Acc. Chem. Res.* **2015**, *48*, 306–316.
- [17] C. B. Caputo, L. J. Hounjet, R. Dobrovetsky, D. W. Stephan, *Science* **2013**, *341*, 1374–1377.

- [18] J. M. Bayne, D. W. Stephan, *Chem. Soc. Rev.* **2016**, *45*, 765–774.
- [19] D. E. Falvey, *Nitrenes and Nitrenium Ions*, Wiley, New York, **2013**, pp. 191–216.
- [20] J. L. Duffy, K. K. Laali, *J. Org. Chem.* **1991**, *56*, 3006–3009.
- [21] S. Moebis-Sanchez, G. Bouhadir, N. Saffon, L. Maron, D. Bourissou, *Chem. Commun.* **2008**, 3435–3437.
- [22] G. A. Olah, J. A. Olah, N. A. Overchuk, *J. Org. Chem.* **1965**, *30*, 3373–3376.
- [23] F. Dielmann, O. Back, M. Henry-Ellinger, P. Jerabek, G. Frenking, G. Bertrand, *Science* **2012**, *337*, 1526–1528.
- [24] Y. Tulchinsky, M. A. Iron, M. Botoshansky, M. Gandelman, *Nat. Chem.* **2011**, *3*, 525.
- [25] Y. Tulchinsky, S. Kozuch, P. Saha, M. Botoshansky, L. J. W. Shimon, M. Gandelman, *Chem. Sci.* **2014**, *5*, 1305–1311.
- [26] Y. Tulchinsky, S. Kozuch, P. Saha, A. Mauda, G. Nisnevich, M. Botoshansky, L. J. W. Shimon, M. Gandelman, *Chem. Eur. J.* **2015**, *21*, 7099–7110.
- [27] A. Pogoreltsev, Y. Tulchinsky, N. Fridman, M. Gandelman, *J. Am. Chem. Soc.* **2017**, *139*, 4062–4067.
- [28] M. Mehta, J. M. Goicoechea, *Angew. Chem. Int. Ed.* **2020**, *59*, 2715–2719; *Angew. Chem.* **2020**, *132*, 2737–2741.
- [29] I. Avigdor, A. Pogoreltsev, A. Kaushanski, N. Fridman, M. Gandelman, *Angew. Chem. Int. Ed.* **2020**, *59*, 23476–23479; *Angew. Chem.* **2020**, *132*, 23682–23685.
- [30] D. Shimizu, K. Fujimoto, A. Osuka, *Angew. Chem. Int. Ed.* **2018**, *57*, 9434–9438; *Angew. Chem.* **2018**, *130*, 9578–9582.
- [31] J. L. Zhou, L. L. Liu, L. L. Cao, D. W. Stephan, *Angew. Chem. Int. Ed.* **2018**, *57*, 3322–3326; *Angew. Chem.* **2018**, *130*, 3380–3384.
- [32] S. S. Ullah, C. Kashyap, A. K. Guha, *ChemistrySelect* **2018**, *3*, 6715–6718.
- [33] J. Zhou, L. L. Liu, L. L. Cao, D. W. Stephan, *Chem. Commun.* **2018**, *54*, 4390–4393.
- [34] A. E. Waked, R. O. Memar, D. W. Stephan, *Angew. Chem. Int. Ed.* **2018**, *57*, 11934–11938; *Angew. Chem.* **2018**, *130*, 12110–12114.
- [35] **2018**, TURBOMOLE, version 7.3, See <http://www.turbomole.com>, TURBOMOLE GmbH, Karlsruhe.
- [36] J. Tao, J. P. Perdew, V. N. Staroverov, G. E. Scuseria, *Phys. Rev. Lett.* **2003**, *91*, 146401.
- [37] S. Grimme, *Chem. Eur. J.* **2012**, *18*, 9955.
- [38] S. Grimme, J. Antony, S. Ehrlich, H. Krieg, *J. Chem. Phys.* **2010**, *132*, 154104.
- [39] S. Grimme, S. Ehrlich, L. Goerigk, *J. Comput. Chem.* **2011**, *32*, 1456–1465.
- [40] P. Deglmann, K. May, F. Furche, R. Ahlrichs, *Chem. Phys. Lett.* **2004**, *384*, 103.
- [41] F. Weigend, M. Häser, H. Patzelt, R. Ahlrichs, *Chem. Phys. Lett.* **1998**, *143*, 294.
- [42] F. Weigend, F. Furche, R. Ahlrichs, *J. Chem. Phys.* **2003**, *119*, 12753.
- [43] F. Weigend, R. Ahlrichs, *Phys. Chem. Chem. Phys.* **2005**, *7*, 3297–3305.
- [44] K. Eichkorn, F. Weigend, O. Treutler, R. Ahlrichs, *Theor. Chem. Acc.* **1997**, *97*, 119.
- [45] **2015**, COSMOtherm, Version C3.0, Release 16.01, COSMOlogic GmbH & Co., Leverkusen, Germany.
- [46] F. Eckert, A. Klamt, *AIChE J.* **2002**, *48*, 369–385.
- [47] A. Klamt, G. Schüürmann, *J. Chem. Soc. Perkin Trans.* **1993**, 799.
- [48] F. Weigend, *Phys. Chem. Chem. Phys.* **2006**, *8*, 1057–1065.
- [49] Y. Zhao, D. G. Truhlar, *J. Phys. Chem. A* **2005**, *109*, 5656–5667.
- [50] T. Araki, M. Hirai, A. Wakamiya, W. E. Piers, S. Yamaguchi, *Chem. Lett.* **2017**, *46*, 1714–1717.
- [51] F. H. Allen, O. Kennard, D. G. Watson, L. Brammer, A. G. Orpen, R. Taylor, *J. Chem. Soc. Perkin Trans. 2* **1987**, S1–S19.
- [52] G. C. Welch, R. R. S. Juan, J. D. Masuda, D. W. Stephan, *Science* **2006**, *314*, 1124–1126.
- [53] G. C. Welch, J. D. Masuda, D. W. Stephan, *Inorg. Chem.* **2006**, *45*, 478–480.
- [54] A. Kozma, G. Gopakumar, C. Fares, W. Thiel, M. Alcarazo, *Chem. Eur. J.* **2013**, *19*, 3542–3546.
- [55] P. W. Antoni, T. Bruckhoff, M. M. Hansmann, *J. Am. Chem. Soc.* **2019**, *141*, 9701–9711.
- [56] D. Rottschäfer, B. Neumann, H. G. Stämmler, M. van Gastel, D. M. Andrada, R. S. Ghadwal, *Angew. Chem. Int. Ed.* **2018**, *57*, 4765–4768; *Angew. Chem.* **2018**, *130*, 4855–4858.

Manuscript received: November 2, 2020

Accepted manuscript online: November 2, 2020

Version of record online: January 14, 2021